Future Energy
Open Access Journal
ISSN 2832-0328

February 2026| Volume 05 | Issue 01 | Pages 41-52

Journal homepage: https://fupubco.com/fuen

https://doi.org/10.55670/fpll.fuen.5.1.5

Future Publishing LLC

Article

Ammonia as a hydrogen carrier: LES of ammonia-solid fuel firing at varying air staging ratios

Mohammad Nurizat Rahman[1]*, Muhamad Shazarizul Haziq Mohd Samsuri[2], Suzana Yusup[3], Ismail Shariff [2]

[1]Energy Markets and Strategy, Energy Systems, DNV, 118227 Singapore
[2]Generation Unit, Generation and Environment, TNB Research, Kajang, Selangor, 43000, Malaysia
[3]Faculty of Engineering and Technology, Sunway University, Selangor, 47500, Malaysia

ARTICLE INFO

Article history:
Received 02 October 2025
Received in revised form
17 November 2025
Accepted 15 December 2025

Keywords:
Large Eddy Simulation (LES), Solid fuel, Coal, Ammonia, Power Generation,
Air-staging combustion

*Corresponding author
Email address:
mohammadnurizatrahman@gmail.com

DOI: 10.55670/fpll.fuen.5.1.5

ABSTRACT

Hydrogen carriers, such as Ammonia (NH_3), is anticipated to be used as a carbon-free alternative for solid fuels, such as coal. Hence, the effect of air staging ratio (ASR) on emissions from NH_3 co-firing with sub-bituminous coal was numerically investigated in a small-scale coal combustor via a Large Eddy Simulation (LES) method. The validation with experimental data demonstrated a difference in nitrogen oxides (NO_x) and temperature profiles of less than 10 %. Carbon dioxide (CO_2) and sulphur dioxide (SO_2) levels are decreasing as the NH3 percentage rises, but ASR has minimal influence. Increasing the ASR from 20 to 60 % resulted in NO_x reduction, except for 60 calorific (cal.) % NH_3, where NO_x began to grow at ASR 60 %. In the said case, peak temperature was recorded in the over-fire Air (OFA) zone due to considerable unburned carbon (UC) oxidation, resulting in an increase in thermal NO_x. Due to oxygen deficiency, coal volatiles and NH_3 are thought to burn in the firing zone due to dominant devolatilization, resulting in significant UC/char oxidation in the OFA zone. Overall, with proper ASR tuning, NH_3 co-firing can produce low CO_2, SO_2, and NO_x, and existing coal-fired utility ASR technology can be used.

1. Introduction

Nowadays, the electricity sector accounts for a significant share of worldwide carbon dioxide (CO2) emissions [1-2], primarily because coal-fired thermal power plants supply a substantial share of global electricity demand, owing to their large reserves and affordability [2-6]. It is a known fact that coal-fired thermal power plants emit more CO2 than other generation systems [7], since coal has a relatively higher carbon content than almost all other fossil fuels [8]. And it serves as one of the main anthropogenic CO_2 emission sources [9], accounting for 41 % of worldwide CO_2 emissions in 2023 [10]. A reduction in greenhouse gas (GHG) emissions is critical as a key control measure for climate change issues, and it is now becoming a worldwide accord [9-13]. The attainment of a sustainable society is extensively spoken about, and the pressure on coal-fired utilities to decarbonise is heightening [5]. At the UN's Climate Change Conference (COP26), more than 40 nations made pledges to abandon coal. Despite the excitement surrounding the net-zero carbon transition, the global energy crisis in recent years has led to a rush for coal demand once more, demonstrating that the rapid switch to renewable energy is, in fact, more difficult than anticipated. One of the solutions to this issue is to gradually phase out coal, so that there is an adequate amount of time for low- and/or zero-carbon technologies to reach economies of scale [2]. Therefore, while waiting for these technologies and their associated supply chains to fully mature, decreasing negative emissions from existing coal-fired thermal power plants is critical for reducing the carbon footprint and eventually establishing the targeted net-zero society [9-10]. Therefore, various techniques are being established to reduce CO_2 emissions from the said plants, including integrated gasification combined cycle (IGCC), ultra-supercritical technology [10], oxy-fuel combustion, carbon capture and storage (CCS) [7], double reheat technology [10], and the use of low-/zero-carbon fuels [11]. When it comes to employing these types of fuels, biofuels (such as biogas and biomass) are appealing fuels for co-firing applications. Yet, variability in harvesting periods indicates fluctuations in feedstock supply and presents significant hurdles for both operations and market sentiment. Carbon-free fuels, such as hydrogen, are another option, expected to play an increasingly important role in creating a net-zero society, especially in hard-to-abate sectors [11-15]. However, owing to its unique properties [11], the storage and transportation of hydrogen remain relatively complex

[13,16]. Hydrogen carriers, such as ammonia (NH_3), are effective alternatives to pure hydrogen, as demonstrated in a report by Rahman [13], owing to their relatively high hydrogen density compared with other hydrogen carriers, such as organic hydrides [16-17]. Additionally, NH_3 is a desirable vector for hydrogen because it retains roughly 90% of the energy from the hydrogen feedstock and is much easier to store due to its ease of liquefaction [18]. Having said that, NH_3 is an enabler of the hydrogen economy, not a competitor [19]. Furthermore, as a fuel, NH_3 can be employed in existing plant-related combustion systems without the need for a procedure to extract its hydrogen content [18], albeit with tuning works to be done where necessary. NH_3 has been regularly and widely employed as a denitrification material in boilers and plants. The latest movement in decarbonising the shipping industry with NH_3 as a marine fuel is an obvious indication of some of its benefits that can be potentially adapted to power generation systems, such as production scalability, a comparatively adequate energy density with relatively simple storage needs as opposed to pure H_2, and secured usage in existing industrial processes. NH_3 is already an essential commodity chemical worldwide, with a mature storage and distribution supply chain that is becoming increasingly crucial to vital aspects of global society, such as the fertiliser industry [17]. As such, infrastructures for NH_3 storage and delivery are well developed [3, 12], and its initial and operational costs are expected to be relatively lower than those of other low-carbon/carbon-free fuels and hydrogen carriers [7], with several techno-economic studies indicating that it has the potential to be the lowest cost zero-carbon option. Hence, NH_3 could be a preferable candidate for widespread use in the future because it is both a hydrogen carrier and a potential replacement for conventional fossil fuels. Hence, it is clear that interest in NH_3 as an electricity-generated component is growing, especially with its prospect as a crucial fuel/feedstock for decarbonising power generation [2].

Co-firing of coal and NH_3 has recently been regarded as a promising method for minimising CO_2 emissions from coal-fired thermal power plants [17]. For the production of NH_3 as a fuel, the "blue NH_3" is expected to be created using CCS to capture carbon emissions [10]. The "green NH_3" could be produced from hydrogen electrolysis from water, utilising the excess renewable electricity (e.g., wind and solar power) [9]. Hence, “green NH_3” is a derivative renewable fuel that functions as a transporter and a storage option for renewable energy [17]. At the same time, it is important to note that the reduction in emissions from NH_3 co-firing is also highly affected by the NH_3 production method [18]. Yet, NH_3 co-firing remains one of the most realistic and appealing options compared to most strategies for fuel blending scenarios [19]. Co-firing methods aim to maximise the utilisation of facilities in existing coal-fired power plants, potentially reducing resource waste and financial/opportunity losses due to power plant early retirement [20]. Moreover, reducing the carbon content of the main fuel stream (in this case, coal) could help cut CO_2 emissions. However, given the limited capacity of NH_3 production facilities worldwide, it is unlikely that NH_3 will fully replace coal in the short to medium term [3]. Possibly in the future, especially in the scenario of NH_3 yield sees an exponential increase due to its use as a hydrogen carrier (combined with government fuel incentives), the associated cost of NH_3 procurement has the potential to fall even further, and it can thus be used as one of the main energy vectors for power generation systems [7]. By utilising green NH_3 as a carbon-free fuel, the integration of existing coal-fired power plants and low-carbon renewable options could be realised, providing an essential engineering pathway for a potentially cleaner coal-fired power generation [10]. Thus, at the moment, co-firing NH_3 with pulverised coal in a boiler is seen as a quick and viable means of effectively lowering CO_2 emissions from these systems, as the world waits for the eventual full phase-out of coal-fired power plants [17].

Despite this, co-firing NH_3 in coal-fired boiler systems could result in elevated nitrogen oxide (NO_x) emissions, owing to its much higher fuel-nitrogen content [9, 12]. These impacts must be investigated in advance, including their emissions and combustion aspects, if NH_3 co-firing is to be widely used in the future. Various organisations worldwide have researched the combustion properties of NH_3 [7]. In the context of combustion assessments, comprehensive data on NH_3 flame propagation across varying operational scenarios aid combustion dynamics assessment and the development of comprehensive reaction mechanisms [12, 16].

Recent advances in research on NH_3 co-firing technology with pulverised coal have been published [3,20]. IHI Corporation, for instance, successfully tested NH_3 co-firing in a pulverised coal combustor system (10 MW size), with NH_3 accounting for 20% of the co-firing ratio. Moreover, the results from these experimental works have demonstrated that for the case of NH_3 co-firing, unburned carbon (UC) in fly ash and NO_x emission could be comparable to those in the scenario of full coal firing, if a proper NH_3 injection technology is adopted. In separate experimental research, the characteristics of pulverised coal+NH_3 co-firing were explored in detail via a horizontally shaped single burner with the feeding rate of 100 kg/hr (coal) [3]. Their results have shown that when the NH_3 was injected from the burner’s centre with NH_3 of 20 cal.%, NO_x concentration in the flue gas has been seen to be elevated by roughly 20 % from the pure coal firing case, and UC in fly ash increased in a moderate manner. These findings suggest that controlling/tuning NH_3-coal co-firing while preserving both flame stability and NO_x emissions is a significant challenge that requires further research to achieve acceptable combustion characteristics.

Tuning the air staging ratio (ASR) is another potential approach for decreasing NO_x emissions when co-firing coal and NH_3. This is the same strategy employed in existing coal-fired power plants, where airflow is distributed via the combustion air and then separated into the burner zone and the over-fire air (OFA) zone above the burner regions [21-22]. The existing air staging system in most coal-fired utility furnaces is a technical advantage. As a result, its start-up and operating costs are expected to be relatively low, as it requires essentially no alteration to the existing coal-fired power system. The only significant change in co-firing NH_3 is at the burner, where a novel NH_3-co-fired burner is required to inject NH_3 with coal [20]. While several studies have examined the co-firing of coal and NH_3 to evaluate its combustion and emission properties, there have been very few investigations into the effects of ASR on these properties. Moreover, a number of important works on NH_3 co-firing

mostly assumed an ideal reactor network model [4, 5, 7, 9, 12]. This assumption is known to neglect the 3D effects of fluid dynamics. Weng [5], for instance, examined the presence of sulphur and alkali species in NH_3 conversion processes in a post-flame environment using ideal reactor networks (Chemkin PRO software), with a focus on the characteristics of NO emissions and the slip of NH_3 in flue gases.

Despite the fact that NH_3 and low-rank coals have comparable energy density [19], it is clear that important NH_3 properties, for example its relatively low laminar burning velocities and energy [16, 23], as well as elevated ignition energies and high auto-ignition temperatures [19], make it more difficult to combust NH_3 efficiently and achieve the operational and combustion performances required by existing coal-fired power plants. In fact, more assessment is necessary before NH_3 is used in existing coal-fired power plants to better understand its combustion and emission properties, mainly through further research on the kinetics and fluid dynamics of NH3 co-firing/full-firing, to aid flow tuning, such as ASR control.

One viable option is computational fluid dynamics (CFD), which can be a useful tool for detailed investigations of the impact of ASR on NH_3 co-firing. Subsequently, it can aid in the tuning of the ASR for actual coal-NH_3 firing for NO_x reduction in power plants. CFD has been frequently utilised to examine heat transmission and combustion dynamics in pulverised coal-fired utility furnaces. Zhang [3], for instance, used CFD approaches to examine the impact of NH_3 ratio on coal+NH_3 co-firing in a pulverised coal combustor facility. The modelling findings were compared with experimental data on NO_x, CO_2, and UC levels. However, when compared to NO_x readings from experimental data, the modelling approaches that use the Reynolds-averaged Navier-Stokes (RANS) model to resolve turbulence flow produced a 35 % and 47 % difference in NO_x and UC levels, respectively.

Cardoso [2] has also used one of the RANS-based models, the *k*- realizable model, to investigate NH_3 and biomass co-firing in a pilot-scale fluidised bed reactor system. The predicted CO_2 and NO emissions from coal+biomass co-firing were compared to the actual CO_2 and NO emissions from coal+biomass co-firing experiments. While the validations show reasonable agreement in terms of trend, there is no direct validation with real coal-NH_3 co-firing. Therefore, it is still not entirely safe to assume that it can reliably simulate coal-NH_3 co-firing when the validation basis is for different fuel blends (coal-biomass). Furthermore, post-processing is the most commonly used approach for NO_x modelling, in which the main gas compositions, temperature, and velocity distributions are first obtained from combustion numerical calculations; then NO_x-related reactions are added [3]. As a result, it is advised to use the combustion simulation parameter to evaluate a reasonable validation. Furthermore, actual NH_3 co-firing test data should be used as a validation benchmark.

In terms of resolving turbulence flow, while the use of the RANS model is beneficial to account for the accuracy and efficiency of the computational processes of NH_3 co-firing [2], there is still more research required to fully comprehend the coal-NH_3 flame dynamics and its associated emissions, which can only be achieved through the use of Large Eddy Simulation (LES). The key advantage of LES over RANS approaches is that it treats turbulence-chemistry interactions (TCI) more realistically [24]. As a result, higher fidelity to simulation results can be achieved. Through the low-pass filtering method, the LES reduces the computational burden by ignoring small length scales that require significant computational effort. Instead, the effect of these small length scales will be modelled using sub-grid scale models [25].

Therefore, LES is a powerful algorithm with a good trade-off between reliable combustion dynamics predictions and computational cost. While LES has been commonly used for NH_3 combustion simulations, the majority of these studies have been focused on co-firing with gaseous fuel, primarily natural gas and methane (CH_4) [26-28]. The use of LES for coal+NH_3 co-firing research is still lacking. Furthermore, the effect of varying ASR on NH_3 co-firing must be studied further for future implementation in coal-fired power plants. Hence, reliable prediction of flame structures, temperature dynamics, and NO_x levels is an important goal in the numerical modelling of coal+NH_3 co-firing via LES in order to provide a holistic risk assessment for coal+NH_3 co-firing at varying ASRs. As a result, in this study, CFD assessments using a detailed LES were performed to examine the effects of NH_3 co-firing on emissions in a small-scale coal combustor facility at various ASRs. Among the studied pollutants are CO_2, SO_2, and NO_x. Sub-bituminous coal rank was used since it is the most commonly used coal rank in Malaysia's coal-fired power plants [29-30]. The prediction accuracy of the CFD approach was first evaluated by comparing it to actual testing data from the pulverised coal combustor testing facility.

2. Experimental setup

The coal+NH_3 co-firing test was carried out in TNB Research's pulverised coal combustor facility, as shown in Figure 1. The thermal input of 150 kW is employed for the co-firing assessment. NH_3 was inserted radially and concentrically from the centre of the coal injector burner, allowing direct mixing with the entering coal and air. This is also to lower the flow velocity of NH_3, allowing for a longer residential mixing time with the coal+air mixture. The coal combustor facility has been built with a flue gas analyser, K-type thermocouples at combustor sections, and a single swirl burner. The air and fuel inlets, the main combustion section, the heat exchanger, and the cyclone are the main parts of the combustor.

The facility also includes a high-temperature glass window for viewing the flame profile and temperature measurements. Within the facility, the embedded combustor is configured in an L-shape to simulate a typical coal-fired boiler layout. This allows for the distinction between radiation, where the high-temperature combustor/flame zone occurs, and convection zones. The coal sample was transported using primary air (PA). Another flow of air, known as secondary air (SA), acts as an oxidising component for the primary combustion process. Throughout the test program, the PA flow rate was held constant at 9 Nm^3/hr, while the coal, SA, and NH_3 volume flow rates were calculated on a calorific/thermal input basis and maintained at 150 kW. The combustor main body, or the longer section of the L-shape, is made up of four tube sections that measure 3.3 m in length and have an internal diameter of 0.6 m each. Each tube section contains one K-type thermocouple for temperature measurement. Section 1 is upstream, and Sections 2, 3, and 4

come after it. The downstream part of the combustor (the shorter length) is about 0.91 m long and has an internal diameter of 0.3 m.

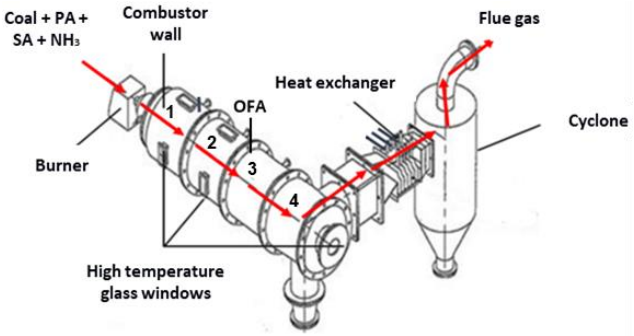

Figure 1. TNB Research's pulverised coal combustor facility

The gas temperatures and compositions at the combustor outlet, comprising CO_2, SO_2, and NO_x, were constantly measured. One of the key aspects of ensuring the success of the testing is to ensure that the temperature from the combustion process within the combustor reaches a sufficiently high temperature condition and then maintains that temperature condition throughout the testing process so that it can mimic the actual temperature condition within the combustion zone of the actual boiler temperature condition. Hence, to achieve this flame temperature, liquefied petroleum gas (LPG) was also fed at a certain range of mass flow rate, roughly 2 kg/hr, with manual flow rate tuning required intermittently to maintain the desired temperature. The presence of NH_3 was also assessed in the flue gas via a detector tube to ensure that no slip of NH_3 occurred. Discharge of NH_3 into the surrounding area is prohibited due to its toxicity [20]. For modelling validation purposes, out of all the testing cases that were done, one test case of pure coal firing and one test case of NH_3 co-firing with a 60 cal.% proportion were selected. The ASR (fraction of OFA) in both of these cases was around 20 %. The properties of the fuels utilised in experiments and numerical studies are shown in Table 1.

3. Numerical setup

CFD techniques were used to simulate the combustion dynamics of pure coal firing and NH_3 co-firing at various ASRs and NH_3 co-firing ratios. ANSYS FLUENT 19.0 was used, and the majority of the default CFD solvers and models were already embedded.

Yet, a new model establishment was needed to account for coal kinetics. The coal-firing simulation accounts for three key stages of the coal combustion process: devolatilization of coal, the subsequent conversion/reaction of char, and volatile reactions (from volatiles released during early devolatilization). The coal network model and the coal database from TNB Research's analytical fuel laboratory were used to determine the composition of volatiles and the corresponding rate constants for coal devolatilization. Our prior studies [29-30] show the chemical reactions and coal combustion models employed in the current CFD assessments. The compressible and reacting Navier-Stokes (NS) equations were used in the numerical model. The pressure-based solver was used to solve the governing equations. Turbulence was solved using the Large Eddy Simulation (LES) model [31]. Wan [32] and Sun [33] provide detailed information on the formulations utilized in the NS equations and LES model for coal combustion. All of the equations were discretised using second-order upwind methods. The coal particle trajectories were traced via a Lagrangian approach, which took into account turbulent dispersion factors in the coal trajectories, an important consideration due to the turbulence mixing of the coal that occurs in the combustor facility. Another consideration is radiation, which was simulated using the discrete ordinate (DO) approach. The radiation model setup includes discretisation, which includes an angular direction of 5 divisions, as well as polar and azimuthal orientations of 3 pixels each. The weighted-sum-of-gray-gases model (WSGGM) [3] was used to predict gas emissivity.

Within the entire CFD frameworks, a different method known as a post-processing technique was employed to predict NO_x emissions from the simulated combustion processes of these fuels. The technique first allowed all combustion iterations to occur, during which all key modelling results were obtained, including temperature, major gas composition, and velocity distributions. Then, reactions of hydrogen cyanide (HCN), NH_3, thermal NO_x, and the eventual NO_x reduction by released/residual char were incorporated after these key iterations in the combustion computation had finished. Having said that, it occurred during post-processing, not during the main processing. Accordingly, NO_x-related species such as NO, NH_3, HCN, O, hydroxide (OH), and N were computed at this stage. Turbulence, flow, other major gas compositions such as CO_2, oxygen, hydrogen, and carbon monoxide (CO), as well as energy and radiation equations, were already solved during the main processing phase. Figure 2 summarizes the calculation approaches for the kinetics of coal-NH_3 combustion and the corresponding NO_x emissions.

Table 1. Fuel properties

Proximate analysis, wt. %, ad., coal (TM-Total moisture, VM-Volatile matter, FC-Fixed carbon, AC-Ash content)				Ultimate analysis, wt. %, ad., coal (C-Carbon, H-Hydrogen, N-Nitrogen, O-Oxygen, S-Sulphur)					GCV- Gross Calorific Value, ad., coal (kcal/kg)		
TM	VM	FC	AC	C	H	N	O	S	Coal A	NH_3	LPG
24	41	39	2	68.7	4.4	0.9	23.7	0.2	6,449	5,374	11,775

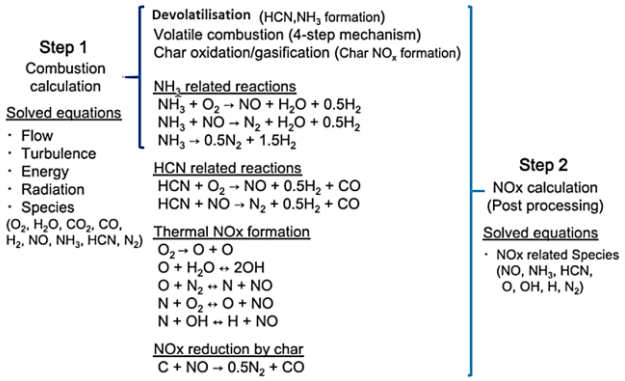

Figure 2. Calculation approaches for the coal-NH_3 combustion kinetics and NO_x

Table 2 depicts the main conditions of simulated cases. This study included 16 cases. The same heat input utilised in the experiment was employed in all numerical cases. As previously stated, the co-firing ratio was calculated on a calorific/thermal input basis and set at 150 kW. The coal, NH_3, and LPG flow rates are shown in Table 2. All cases have an equivalence ratio (Ø) of 1, indicating a stoichiometric condition. The combustion air (PA + SA) flow rate was determined using the coal/NH_3/LPG ratio at a stoichiometric condition. The coal-to-NH_3 co-firing ratio was varied, and NH_3 co-firing was increased from 0 to 60 cal.% at various ASRs. While the maximum ASR for a coal-fired air-staged combustion system is typically no more than 40 % due to fuel burnout issues, the ASR was set to 60 % for the current assessment to gain combustion insights for future ASR tuning of coal-NH_3 firing in actual coal-fired power plants. The overall ratio of coal+NH_3 to LPG was kept constant to ensure a constant LPG flow rate, with the LPG ratio kept at 27 cal.% and the rest being coal+NH_3 ratio (83 cal.%).

The exact drawing of the combustor facility was used to generate the 3D model of its computational domain, which was later discretised mainly with hexahedral meshes using the Assembly Meshing method. A mesh-independent test was performed to ensure that the modelling results were not affected by the number of meshes. Table 3 presents the properties of the meshes used in the computational domain. Since the quality of meshes affects the spatial discretisation error, meshes were generated with both skewness and orthogonality taken into account to reflect overall mesh quality. Orthogonality indicates how closely the angles between consecutive mesh faces approach the ideal mesh angle. The scale of orthogonal quality ranges from 0 to 1, with 1 indicating the highest quality [34]. Skewness reflects how close the mesh is to an optimal equiangular mesh.

Heavily skewed meshes and their corresponding faces are unsuitable, as the governing equations are solved under the assumption that meshes are roughly equiangular. Skewness also ranges from 0 to 1, where values close to zero have the slightest deviation from a normalised equiangular angle [34]. All meshes were optimised to achieve high quality across both mesh quality metrics, as shown in Table 3.

The predicted velocity and NO_x (case C12) at the coal combustor outlet as the mesh count changes are shown in Figure 3. When the mesh number is increased from 2.412 million to 4.171 million, NO_x and velocity change little, with variations of less than 1 %. Hence, 2.412 million meshes were selected for the coal combustor domain.

Figure 4 illustrates the mesh-independent model of the coal combustor's computational (fluid) domain, as well as the boundary inlet details. Since the upstream region (inlet) entails intricate reactions and mixing of NH_3, coal, air, and LPG, a finer mesh was generated in that zone.

Table 2. Primary conditions of simulated cases

Cases	ASR (%)	Coal + NH_3 = 82 cal.%		LPG (cal.%)	Coal (kg/hr)	NH_3 (kg/hr)	LPG (kg/hr)	Ø
		Coal (cal.%)	NH_3 (cal.%)					
C10	0	100	0	27	10.00	0.00	2.00	1
C12	20	80	20		8.00	2.40		
C13	40	60	40		6.00	4.79		
C14	60	40	60		4.00	7.19		
N20	0	100	0		10.00	0.00		
N22	20	80	20		8.00	2.40		
N23	40	60	40		6.00	4.79		
N24	60	40	60		4.00	7.19		
N30	0	100	0		10.00	0.00		
N32	20	80	20		8.00	2.40		
N33	40	60	40		6.00	4.79		
N34	60	40	60		4.00	7.19		
N40	0	100	0		10.00	0.00		
N42	20	80	20		8.00	2.40		
N43	40	60	40		4.00	4.79		
N44	60	40	60		4.00	7.19		

Table 3. Mesh characteristics

Average element size (mm)	Meshes, 10^6	Orthogonal quality	Skewness
300	0.069	0.916	0.094
200	0.081	0.936	0.079
100	0.120	0.971	0.051
50	0.162	0.990	0.024
30	0.273	0.991	0.041
20	0.530	0.993	0.037
15	0.958	0.992	0.025
13	1.425	0.990	0.016
10	2.412	0.995	0.014
8	4.171	0.996	0.019

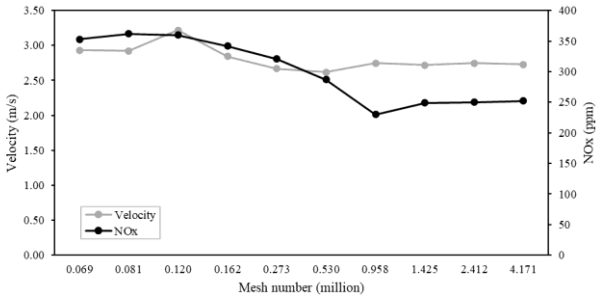

Figure 3. Predicted velocity and NO_x at varying mesh counts (location: combustor outlet)

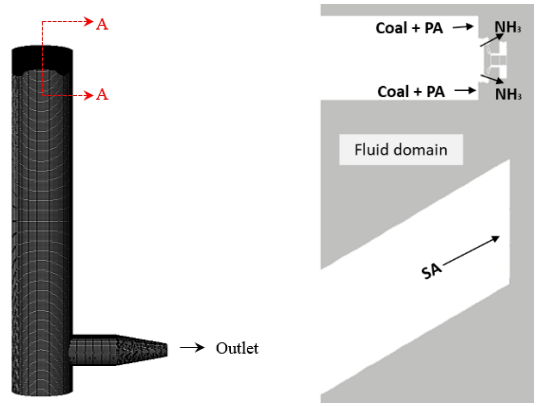

(a) (b)

Figure 4. Coal combustor domain with (a) mesh model and (b) boundary inlets in plane AA view

4. Results and discussion

Figures 5 and Figure 6 display the validation results for NOx levels and temperature profiles from experiments and numerical simulations. The numerical results from the simulated cases with varied ASRs were thoroughly evaluated in subsequent sections based on predicted CO_2, SO_2, and NO_x. For validation, NO_x and temperature profile data from experimental coal firing and NH_3 co-firing were compared to the numerical results from cases C12 and N42, respectively.

4.1 Validation I: NO_x concentrations

According to Figure 5, NH_3 co-firing results in higher NO_x concentrations at the combustor exit in both the simulation and the experiment than in coal combustion. Based on the validation cases, the NOx concentrations in the coal-firing and NH_3-cofiring cases are 265 and 1,573 ppm, respectively (according to the experimental results). Therefore, as the fraction of NH_3 climbs to 60 cal.%, the NO_x concentration increases by around 494 %, roughly five times more than that produced by the pure coal combustion scenario. It is well known that decreasing prompt and thermal NO_x is always challenging in combustion involving carbon-dominant fuels. Yet, it appears that adding NH_3 enhances the likelihood of fuel-bound nitrogen to interact with oxygen in the air, as seen in the experimental results in Figure 5. The synergistic effect of the fuel-bound nitrogen results in a considerable increase in the total NO_x emissions, which consists of fuel, prompt, and thermal NO_x.

According to the numerical results, the established model appears to perform reasonably well when comparing the NO_x results from both the model and the testing, with discrepancies in NO_x concentrations between the two (for both coal firing and NH_3 co-firing) being below 10 %. Despite the model's ability to simulate a broadly similar increasing trend in NO_x emissions when NH_3 co-firing is employed compared to the 100% coal firing case, there remains a slight variation between NO_x values simulated by the established model and the ones obtained from the actual tests. One explanation for the minor discrepancies is that the techniques for NO_x modelling used in this study, as previously mentioned, are based on a method that relies heavily on a set of mechanism that is semi-empirical in basis [3]. Of course, in the actual kinetics process from these fuels' combustion, the reaction pathways for the NO_x production are substantially more intricate, necessitating a greater computing cost to resolve the key chemical kinetics that are involved [12]. Therefore, semi-empirical mechanisms, while excellent for parametric and/or scaling assessments, may not be fully sufficient to provide absolutely correct NO_x emissions. Nonetheless, when compared to the testing data, the simulation results shown in Figure 5 still showed a NO_x difference with testing results below 10 %. Furthermore, quantitatively, it can be observed that the trend in the testing data matches the trend in NO_x emissions simulated by the established numerical model. Hence, adequate validation can be reasonably claimed as the model can model NO_x emissions with reliable accuracy for both pure coal firing and NH_3 co-firing. Safety-wise, it is important to note that the slip of NH_3 was not detected at the outlet of the combustor facility throughout the tests, which can be safely assumed to mean that there are no safety issues related to toxic NH_3 slip being detected.

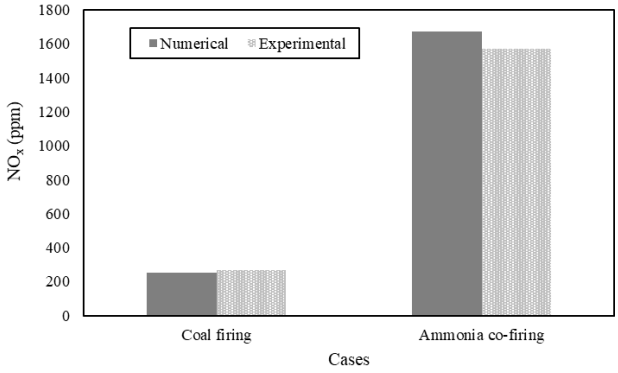

Figure 5. NO_x results from numerical and experimental works (ASR 20 %)

It can be reasonably postulated that this is mainly because of the direction in which the NH_3 was injected into the combustor, where it is injected radially and concentrically from the coal injector's centre at the burner inlet. This allows for a higher residence time for mixing with incoming combustion air and coal, hence reducing the jet velocity of NH_3 entering the combustor. With the combined effects of these higher mixing rates, the potential for NH_3 to escape from the recirculation zone is lower as well (as supported by a previous study [7]). This recirculation zone is important for flame stability in the combustor. Hence, the directional injection factor of NH_3 is potentially the key reason for the inexistence of NH_3 slip.

4.2 Validation II: Temperature profiles

As shown in Figure 6, the one-point temperature in each tube section of the coal combustor testing facility was measured using thermocouples. The testing data showed that the temperature difference (average) between the NH_3 co-firing and 100% coal firing cases varied between 0.9 and 6.1 %. The average difference in numerical data between the two cases ranged from 0.4% to 4.9%. Due to the constant thermal input, differences in temperature were almost negligible in both cases: 100% coal firing and NH_3 co-firing. Of the four tube sections of the combustor, Section 2 had the highest temperature (testing data), and it also had the highest temperature in the modelling assessments. The OFA enrichment between the two middle sections, Sections 2 and 3, which serves as a thermal NO_x mitigation method and also stops the flame front from elongating to reach between Sections 3 and 4, resulted in a significant temperature drop after Section 2. From the experimental data, the maximum temperatures are 1,149 °C for 100% coal firing and 1,121 °C for NH3 co-firing, indicating a measured peak temperature difference of 2.4%. The numerical model predicts maximum temperatures of 1,222 and 1,184 °C for the 100% coal-firing and NH3 co-firing cases, respectively. Therefore, there is a 3% difference in peak temperature between these two fuel scenarios, according to modelling results. Peak temperature differences between testing and numerical results are 5.9 and 5.3 % for 100% coal and NH_3 co-firing cases, respectively.

A possible cause of these minor differences is the calculation of the turbulence-chemistry model in the current CFD frameworks. It is important to note that the turbulence-combustion model used in the current study provides one of the best possible balances between the efficiency and accuracy of reacting flow CFD modelling. However, it remains a known fact that the LES algorithm filters the comparatively small-sized eddies to be modelled purely via the sub-grid formulation [31]. As a result, the current CFD framework does not fully capture the overall range of length scales. This could result in minor regional differences in flame front dynamics and corresponding temperatures.

Still, the peak temperature difference between experimental and numerical results is less than 6 %. Qualitatively, the numerical predictions for the temperature profile positioning and trend nearly match those measured from test data. Therefore, the validation can be considered satisfactory, and the model can reliably predict temperature behaviour in both NH_3 co-firing and 100% coal-firing cases.

4.3 Impacts on CO_2 emission

CO_2 compositions in flue gas changed dramatically when NH_3 was co-fired in the coal combustor, as illustrated in Figure 7. In NH_3 co-firing situations, the fraction of CO_2 in flue gas was much lower than in the coal-fired base case. As anticipated, the CO_2 fraction decreased as the NH_3 co-firing ratio increased. When the NH_3 co-firing ratio reached 60 cal.%, the CO_2 emission dropped to 7.8 % (for 0 % ASR), equal to a 41 % reduction in CO_2 emissions as compared to the coal-fired base scenario. CO_2 emissions fell to 7.9, 8.0, and 8.1 % at ASRs of 20, 40, and 60 %, respectively (co-firing ratio 60 cal.%). This equates to a reduction in CO_2 emissions of 41 to 42 % when compared to the coal-fired base scenario.

The numerical results show that the CO_2 emission ranges for coal firing, 20, 40, and 60 cal.% NH_3 cases are 13.2 to 14.0 %, 11.2 to 12.1 %, 9.7 to 10.5 %, and 7.8 to 8.2 %, respectively. As a result, increasing the percentage of NH_3 in the fuel to 20, 40, and 60 cal.% reduces CO_2 emissions by roughly 13.1, 25.7, and 41.7 %, respectively, when compared to the coal-fired case. Since NH_3 is a carbon-free fuel, replacing coal with NH_3 reduces CO_2 emissions directly, with the decline ratio roughly equalling the fuel replacement ratio on a heating value basis.

The percentage difference between the lowest and highest CO_2 emissions when the ASRs were varied is less than 10% in all cases shown in Figure 7. Hence, the difference in ASR has no substantial effect on CO_2 emissions. While greater ASRs will result in a considerable increase in UC from the main combustion zone due to the lack of oxygen caused by reduced airflow, the remaining airflow was subsequently injected into the OFA zone to complete the oxidation of UC to generate CO_2. Since the combustion temperature has a relatively lesser effect on CO_2 production than thermal NO_x [35], the considerably lower temperature of injected OFA could still complete the oxidation of UC to generate CO_2. Hence, despite the obvious CO_2 decrement as NH_3 increased, the main finding from this assessment is that the staging air element has literally no impact on CO_2 emissions during coal-NH_3 combustion.

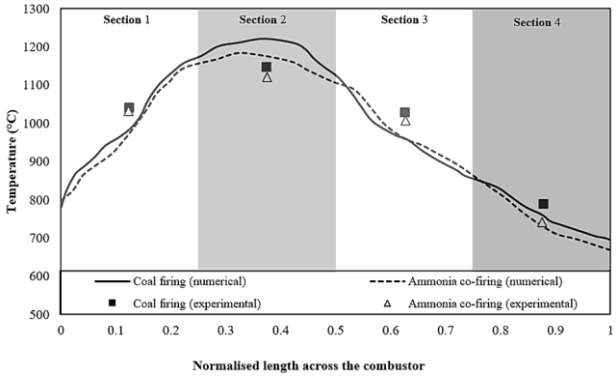

Figure 6. Temperature results from numerical and experimental works (cases C12 and N42)

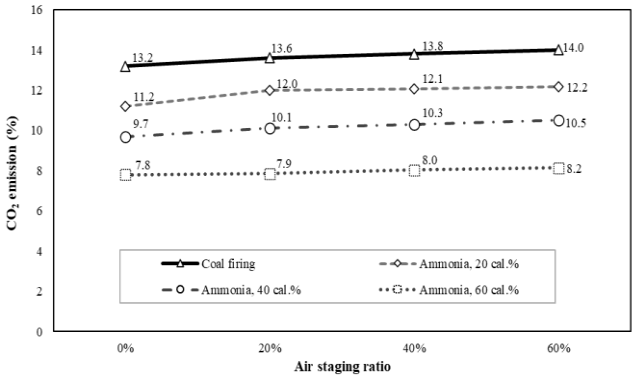

Figure 7. CO_2 data at varying NH3 ratios and ASRs

4.4 Impacts on SO_2 emission

As shown in Figure 8, the SO_2 concentrations in flue gas altered significantly when NH_3 was co-fired in the coal combustor. The concentration of SO_2 in flue gas was substantially lower in NH_3 co-firing scenarios than in the coal-fired base case. As the NH_3 co-firing ratio increased, the SO_2 concentration decreased. When the NH_3 co-firing ratio reached 60 cal.%, SO_2 emissions plummeted to 12 ppm (for 0 % ASR), representing a 75 % reduction in SO_2 emissions as opposed to the coal-fired base case.

When the NH_3 co-firing ratio reached 60 cal.%, SO_2 emissions dropped to 13.0, 13.1, and 13.2 ppm at ASRs of 20, 40, and 60 %, respectively. When compared to the coal-fired base scenario, this translates to a 71 to 72 % reduction in SO_2 emissions. The numerical results show that the SO_2 emission ranges for coal firing, 20, 40, and 60 cal.% NH_3 cases are 45.5 to 47.0 ppm, 34.1 to 36.7 ppm, 23.0 to 25.1 ppm, and 12.0 to 13.2 ppm, respectively. Hence, raising the amount of NH_3 in the fuel to 20, 40, and 60 cal.% reduces SO_2 emissions by approximately 24.1, 47.9, and 72.5 %, respectively, as compared to the coal-fired case.

Because this assessment was conducted at a pilot coal combustor testing facility, the injected fuel flow rates are significantly lower than the actual fuel flow rates in coal-fired power plants. As a result, the predicted SO_2 concentration values in Figure 8 are very low in comparison to the actual SO_2 emissions from industrial coal combustion systems such as coal-fired power plants. Moreover, it is crucial to note that the sulphur concentration of the sub-bituminous coal utilised in the current assessment (Table 1) is lower than the sulphur content of common sub-bituminous coals. Hence, the SO_2 concentration in the coal-fired base scenario is already substantially lower. Nonetheless, for parametric analysis, the percentage reduction of SO_2 when NH_3 was co-fired is one of the most relevant research outcomes. NH_3 is not only a carbon-free fuel, but it also contains no sulphur. As a result, increasing the amount of NH_3 has resulted in a significant decrease in SO_2 concentrations due to a lack of sulphur as a portion of coal is replaced by NH_3.

The percentage disparity in SO_2 emissions between the lowest and highest ASRs is likewise less than 10 % in all cases shown in Figure 8. As a result, the variation in ASR has no discernible influence on SO_2 emissions. However, notable discoveries can be found in the coal-fired base case, where no ASR was used. It was predicted that a slightly higher SO_2 concentration would occur in this case. The rise in SO_2 emissions might be explained by the leaner fuel condition (main combustion zone) in the coal firing case, where no ASR was used. With greater oxygen available in the main combustion zone, it reduces the likelihood of other sulphurous substances such as hydrogen sulphide (H_2S), carbonyl sulphide (COS), and carbon disulphide (CS_2) being created, as most of the available oxygen oxidises to become SO_2. This is also corroborated by prior findings that a fuel-rich region will lead to a reduction in SO_2 emissions from coal combustion [35]. As a result, for the coal firing situations depicted in Figure 8, the adoption of an ASR is predicted to result in lower SO_2 emissions than the no staging ratio case due to the fuel-rich condition in the primary combustion zone as oxygen availability decreases.

Furthermore, during coal devolatilization, a portion of sulphur is liberated from the coal as one of the volatiles, and the remainder of sulphur remains within the char (residual of coal after devolatilization) [35]. As a result, sulphur retention in char/UC is suggested to be another explanation for slightly reduced SO_2 in the ASR cases. This is because, in the ASR cases, the fuel-rich zone occurs within the main combustion zone, so the devolatilization intensity decreases, lowering the char combustion intensity, which is mostly affected by volatiles combustion. Hence, in a fuel-rich environment of coal firing, the sulphur in char/UC has the tendency to release a lesser amount of sulphur than in a fuel-lean environment.

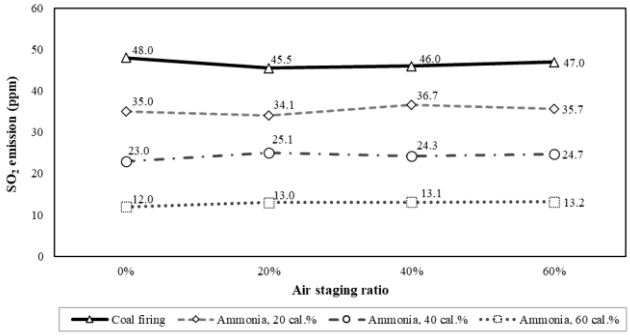

Figure 8. SO_2 data at varying NH_3 ratios and ASRs

4.5 Impacts on NOx emission

The NO_x concentrations in flue gas changed greatly when NH_3 was co-fired in the coal combustor, as shown in Figure 9. NO_x concentrations in flue gas were notably higher in NH_3 co-firing scenarios than in the coal-fired baseline case. The NO_x concentration grew as the NH_3 co-firing ratio increased. When the NH_3 co-firing ratio reached 60 cal.%, NO_x emissions soared to 1,918 ppm (for 0 % ASR), reflecting a staggering 632.06 % increase in NO_x emissions, approximately six times that of the coal-fired base case.

The numerical findings show that the NO_x emission ranges for coal firing, 20, 40, and 60 cal.% NH_3 cases are 250 to 282 ppm, 492 to 895 ppm, 685 to 1,460 ppm, and 1221 to 1918 ppm, respectively. Therefore, compared to the coal-fired scenario, increasing the amount of NH_3 in the fuel to 20, 40, and 60 cal. % increases NO_x emissions by an average of 146.5, 311.1, and 480.2 %, respectively.

However, as the NH_3 co-firing ratio reached 60 cal.%, NO_x emissions reduced to 1,670 and 1,221 ppm for ASRs of 20 and 40 %, respectively. Yet, as soon as the staging ratio for the aforesaid NH_3 co-firing ratio hit 60 %, the NO_x emission began to increase. The NO_x reduction trend is also visible in 20 and 40 cal.% of NH_3 co-firing cases. NO_x emissions were reduced to 672, 532, and 492 ppm in NH_3 20 cal.% co-firing cases with ASR increases of 20, 40, and 60 %, respectively. With an increase in ASR of 20, 40, and 60 % for NH_3 40 cal.% co-firing, NO_x emissions were lowered to 1,383, 793, and 685 ppm, respectively.

Furthermore, with an ASR of 60 %, the NO_x emission from the 20 and 40 cal.% NH_3 co-firing approaches the NO_x emission from the coal firing base case. Using a 60 % ASR, the percentage difference between the coal firing base case and NH_3 co-firing cases was reduced to 74.5 (20 cal.% NH_3) and 142.9 % (40 cal.% NH_3). These percentage differences are much lower than those obtained when no air staging was used, which are 241.6 (40 cal.% NH_3), 457.3 (40 cal.% NH_3), and 632.1 % (60 cal.% NH_3). Therefore, it was expected that the use of air staging would greatly aid in reducing NO_x when NH_3 was co-fired.

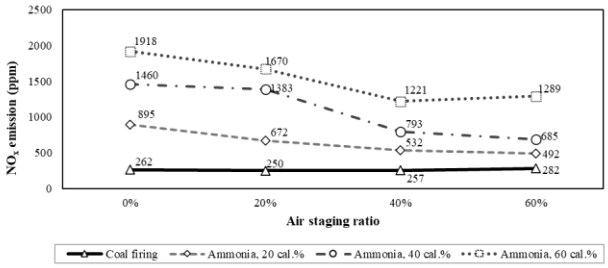

Figure 9. NO_x data at varying NH_3 ratios and ASRs

Adopting a 60 % ASR severely curtailed the airflow for the main combustion zone, resulting in an extremely rich in fuel state with a large deficit in oxygen concentration. As a result, it significantly reduces the oxidation intensity with the nitrogen in fuel, resulting in a reduction in fuel NO_x. Furthermore, the very fuel-rich main combustion zone reduces temperature, which reduces the creation of thermal NO_x [36]. The remaining injected airflow (60 %) is supplied by the OFA technology above the main combustion zone via a separate injector situated above the said zone. The firing process is effectively terminated in this OFA zone. Consequently, the relatively low temperature in the OFA injection zone helps to further reduce the production of thermal NO_x. Furthermore, the injected SA surrounded the core combustion zone. As a result, a relatively low temperature in the oxygen-enriched afterburning zone provides a further reduction in the generation of thermal NO_x. This is a common approach used in coal-fired boiler Low NO_x burners [36]. Previous kinetic studies have also supported the aforementioned findings, revealing that for NH_3 co-firing with coal, thermal NO_x and fuel NO_x are the dominant NO_x types produced [4, 12].

Thus, it can be observed that limiting oxygen availability during the crucial stage of coal devolatilization is the most efficient way to reduce NO_x formation from the NH_3 co-firing. The coal devolatilization is hypothesised to occur primarily in the primary combustion zone due to its relatively short processes as opposed to the char oxidation [30, 37] since the combustion zone in the current coal combustor is relatively smaller than that in the actual coal-fired boiler. Later on in the operation, more air (oxygen) can be introduced by the OFA technology to finish char reactions, lower UC, and maintain high combustion efficiency [22].

However, as the ASR surpasses 40 %, the NO_x reduction gradient begins to decrease for 20 and 40 cal.% NH_3 but begins to climb for 60 cal.% NH_3. Previous research has also indicated that when the ASR crosses a particular quantity, NO_x levels begin to rise [38]. This is because when the ASR exceeds a particular threshold value, a large proportion of NO_x production is repressed at the primary combustion zone, where the air ratio is small. Yet, a significant amount of UC stays in the said position and is burned at the OFA zone to complete its oxidation. Since a substantial quantity of UC is burned in the OFA zone, the combustion intensity increases, causing the nitrogen content in the fuel to oxidize and produce NO_x in the OFA zone. In other words, while the main combustion zone generates the highest temperature along the coal combustor, the high UC content at the OFA zone generates another peak combustion temperature, commonly known as delayed combustion, resulting in nitrogen oxidation in fuel at a high temperature in the OFA zone.

Figure 10 depicts temperature contours within the coal combustor model (excluding the convection zone – shorter length region) at NH_3 60 cal.% at various ASRs. There is a completely visible second temperature peak at the OFA zone, especially at 60 % ASR. Hence, it promotes the development of thermal NO_x at the OFA zone. The temperature distribution near the outlet, where the temperature is higher as opposed to lower/no ASRs, can also indicate delayed combustion at high ASRs. Figure 10 also shows that the flame temperature is higher in the absence of ASR than in its presence, indicating that more oxygen is available to achieve a higher combustion temperature. The flame temperature has been observed to decrease as ASR increases due to a reduction in available oxygen in the main firing area.

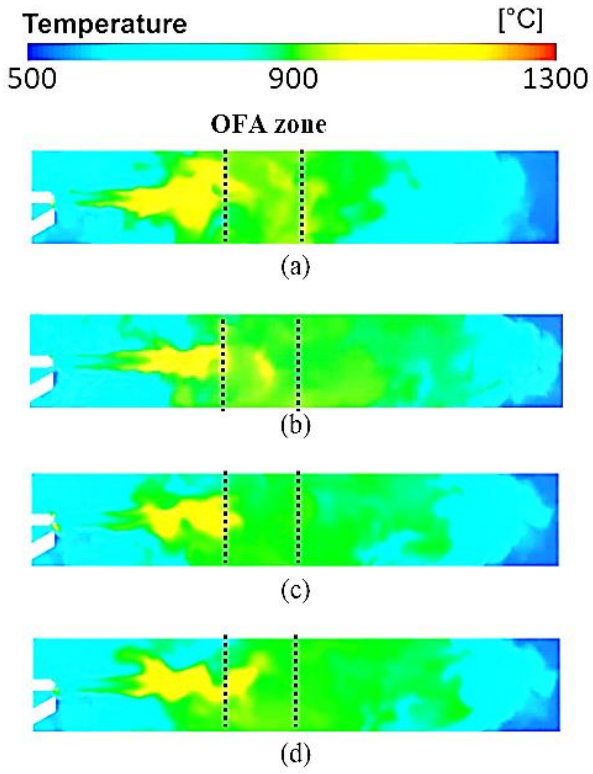

Figure 10. Temperature contours (NH_3 60 cal. %) at (a) 0 %, (b) 20 %, (c) 40 %, and (d) 60 % ASRs

In Figure 9, the degree of ASR has a smaller effect on NO_x emissions in the coal-firing base scenario than in the NH_3 co-firing scenarios. The predicted NO_x levels decreased slightly, from 262 to 250 ppm, as the ASR increased from 0 to 20 % in the coal-fired base scenario. However, when the staging ratio reaches 40% and 60 %, there is a slight increase in NO_x in the coal-firing base scenario. The increase, however, is not as significant as in the NH_3 60 cal.% case. As previously stated, devolatilization occurred primarily in the main combustion zone. Because the char reaction has a faster ignition rate than coal, the VM of coal and NH3 are assumed to burn in the primary firing zone [32], resulting in a slight increase when ASR 40 and 60 % were implemented in the coal firing base scenario. The amount of these components in NH_3 co-firing, however, is greater than in coal firing. Therefore, it is postulated that when NH3 co-firing reaches 60 cal.%, along with a high ASR (60 %), the air-to-VM ratio in the main combustion zone is lower than in the coal-only case. Hence, a substantially larger amount of char/UC remains, which is burned at the OFA position, causing thermal NO_x to be much higher than in the coal firing case.

Furthermore, these findings were supported by a comprehensive kinetics reactor network 0D modelling by Ishihara [7]. Despite the fact that their analysis ignored the impacts of fluid dynamics and 3D characteristics, their kinetics pathway showed that for a relatively high NH_3 co-firing ratio, complete NH_3 reactions cannot be achieved in the primary firing area. As a result, it demonstrates the prospect of nitrogen-related radicals being combusted further upstream in the coal combustor region, such as the OFA zone with significant oxygen availability, as predicted by current numerical assessments. The devolatilization, volatiles reaction, and NH_3 reaction are more prominent in the combustion zone than the char/UC reactions due to the significant amount of VM and NH_3 in 60 cal.% NH_3 co-firing. The aforesaid hypothesis has also been supported by prior research, which indicated that NH_3 co-firing, both in fuel-rich and fuel-lean conditions, promoted coal devolatilization and volatile release [8]. Furthermore, with the use of sub-bituminous coal in the current study, which is known to have a higher VM than common bituminous coals [25], the devolatilization and volatiles reactions will dominate even more. Therefore, the current findings support prior 0D kinetic modelling studies that revealed that NH_3 reactions inhibit char oxidation [7].

5. Conclusion

In the context of reducing CO_2 emissions from pulverised coal-fired boilers, the paper studied the potential of NH_3 to be utilised as a carbon-free substitute for coal, at least partially, to aid in the progressive phase-out of coal. In this research, the co-firing of NH_3 with sub-bituminous coal was numerically studied via a detailed LES assessment at various ASRs in a small-scale coal-fired testing combustor. In-depth insight into predicted emissions, including CO_2, SO_2, and NO_x, was successfully obtained, and an appropriate ASR for a number of NH_3 co-firing percentages was discovered to enable the reduction of such emissions. The prediction accuracy of the model's results was first evaluated by validating it with actual testing data from TNB Research's coal combustor testing facility, which revealed a below 10 % difference in NO_x emissions and temperature results for both 100% coal firing and NH_3 co-firing cases. As a result, the validation can be deemed satisfactory, and the model can forecast the expected emissions with reliable accuracy for both these cases. All in all, the research has demonstrated that coal+NH_3 co-firing can produce low CO_2, SO_2, and NO_x emissions as opposed to pure coal-firing with proper ASR tuning. As the variation of ASRs was studied, important findings regarding emission characteristics were discovered, where the synergistic effect of NH_3 co-firing with coal plays a significant part in the selection of ASR to be used at a specific NH_3 co-firing case. The increase in NO_x when the staging ratio reached 60 % revealed that devolatilization occurred primarily in the main combustion zone due to the smaller firing space compared to actual coal-fired power plants, as well as the shorter devolatilization duration compared to char reaction. As a result, reaction, VM of coal, and NH_3 are assumed to be what burns at the primary firing zone, with the amount of these components in NH3 co-firing being greater than in a pure coal firing scenario. This causes considerable UC oxidation in the OFA zone, which has high oxygen availability, and results in a relatively higher combustion temperature in the OFA zone. These findings contribute to vital information for combustion tuning in actual coal-fired power plants to achieve NH_3+coal co-co-firing and reduce CO_2 emissions. The numerical results also confirmed that NH_3 can be used as an alternative fuel to reduce CO_2 emissions in actual coal-fired power boilers. The air staging method has been shown to provide reduced CO_2, SO_2, and NO_x emissions when the ASR is properly tuned to ensure acceptable staging combustion within the furnace. As a result, existing coal-fired power plant air staging technology can be utilised to provide proper NH_3 co-firing while attaining low NO_x emissions. This is critical information for retrofit setups because it is possible that the only adjustment required is the addition of a new NH_3 burner. However, in the current work, the combustion zone is simplified, and the effects of multiple burners (which actual coal-fired boilers have), such as flame interplay, are not fully examined. Plus, the size of the coal combustor employed is smaller than that of a typical coal-fired utility boiler. When several burners are used, as in commercial boilers, it is expected that estimating the amount of emissions will become more complex due to the presence of additional flame interaction and/or the stronger influence of mixing residence time. Further research can be conducted to investigate the impact of multiple burners and different NH_3 burner designs on emission and combustion characteristics. It is also expected that a higher NH_3 co-firing ratio will be required in the future to accomplish further CO_2 emission reductions. Hence, future research can include an increase in the NH_3 co-firing ratio.

Ethical issue

The authors are aware of and comply with best practices in publication ethics, specifically concerning authorship (avoidance of guest authorship), dual submission, manipulation of figures, competing interests, and compliance with policies on research ethics. The authors adhere to publication requirements that the submitted work is original and has not been published elsewhere in any language.

Data availability statement

The manuscript contains all the data. However, more data will be available upon request from the corresponding author.

Conflict of interest

This work was funded by the TNB Research Seeding Fund (Grant No. TNBR/SF 429/2022). All research activities and analysis associated with this paper were completed by the authors during their respective tenures at TNB Research, regardless of their current affiliations at the time of submission.

References

[1] Cesaro Z, Ives M, Nayak-Luke R, Mason M, Banares-Alcantara R. Ammonia to power: Forecasting the levelized cost of electricity from green ammonia in large-scale power plants. Appl Energy. 2021; https://doi.org/10.1016/j.apenergy.2020.116009

[2] Cardoso JS, Silva V, Chavando JAM, Eusebio D, Hall MJ. Numerical modelling of the coal phase-out through ammonia and biomass co-firing in a pilot-scale fluidized bed reactor. JFUECO. 2022; https://doi.org/10.1016/j.jfueco.2022.100055

[3] Zhang J, Ito T, Ishii H, Ishihara S, Fujimori T. Numerical investigation on ammonia co-firing in a pulverized coal combustion facility: Effect of

ammonia co-firing ratio. Fuel. 2020; https://doi.org/10.1016/j.fuel.2020.117166
[4] Tsukada N, Kinoshita N, Kabuki Y, Taguchi Y, Takashima Y, Tsumura T, Taniguchi M. Role of OH Radical in Fuel-NOx Formation during Cocombustion of Ammonia with Hydrogen, Methane, Coal, and Biomass. Energy Fuels. 2020; https://dx.doi.org/10.1021/acs.energyfuels.0c00356
[5] Weng W, Li Zhongshan, Marshall P, Glarborg P. Participation of alkali and sulfur in ammonia combustion chemistry: Investigation for ammonia/solid fuel co-firing applications. Combust Flame. 2022; https://doi.org/10.1016/j.combustflame.2022.112236
[6] Chen P, Jiang B, Wang H, Gu M, Fang Y, Wang P. Experimental and theoretical calculations study on heterogeneous reduction of NO by char/NH3 in the reduction zone of ammonia co-firing with pulverized coal: Influence of mineral Fe. Fuel. 2022; https://doi.org/10.1016/j.fuel.2021.122374
[7] Ishihara S, Zhang J, Ito T. Numerical calculation with detailed chemistry on ammonia co-firing in a coal-fired boiler: Effect of ammonia co-firing ratio on NO emissions. Fuel. 2020; https://doi.org/10.1016/j.fuel.2020.117742
[8] Zhu J, Liu X, Xu Y, Xu J, Wang H, Zhang K, Cheng X, Yu D. Probing into Volatile Combustion Flame and Particulate Formation Behavior During the Coal and Ammonia Co-firing Process. Energy Fuels. 2021; https://doi.org/10.1021/acs.energyfuels.2c01450
[9] Wang X, Fan W, Chen J, Feng G, Zhang X. Experimental study and kinetic analysis of the impact of ammonia co-firing ratio on products formation characteristics in ammonia/coal co-firing process. Fuel. 2022; https://doi.org/10.1016/j.fuel.2022.125496
[10] Yuan T, Xu Y, Wang C, Gao P, Zhao P, Zhao L, Jin C, Li C, He B. Calculation of CO2 emissions from coal-fired power plants based on OCO-2/3 satellite observations and divergence model: Energy. 2025; https://doi.org/10.1016/j.energy.2024.134303
[11] Chen P, Fang Y, Wang P, Gu M, Luo K, Fan J. The effect of ammonia co-firing on NO heterogeneous reduction in the high-temperature reduction zone of coal air-staging combustion: Experimental and quantum chemistry study. Combust Flame. 2022; https://doi.org/10.1016/j.combustflame.2021.111857
[12] Ishihara S, Zhang J, Ito T. Numerical calculation with detailed chemistry of effect of ammonia co-firing on NO emissions in a coal-fired boiler. Fuel. 2020; https://doi.org/10.1016/j.fuel.2019.116924
[13] Rahman MN, Wahid MA. Renewable-based zero-carbon fuels for the use of power generation: A case study in Malaysia supported by updated developments worldwide. Energy Rep. 2021; https://doi.org/10.1016/j.egyr.2021.04.005
[14] Rahman MN, Ujir MH, Wahid MA, Yasin MFM. A single-step chemistry mechanism for biogas supersonic combustion velocity with nitrogen dilution. J Therm Anal Calorim. 2022; https://doi.org/10.1007/s10973-022-11356-x
[15] Rahman MN, Shahril N, Yusup S. Hydrogen-Enriched Natural Gas Swirling Flame Characteristics: A Numerical Analysis. CFD Lett. 2022; https://doi.org/10.37934/cfdl.14.7.100112
[16] Chen P, Wang H, Jiang B, Wang Y, Gu M, Chen G, Huang X. An experimental and theoretical study of NO heterogeneous reduction in the reduction zone of ammonia co-firing in a coal-fired boiler: Influence of CO. Fuel Process Technol. 2022; https://doi.org/10.1016/j.fuproc.2022.107184
[17] Cardoso JS, Silva V, Eusebio D, Tarelho LAC, Hall MJ, Dana AG. Numerical modelling of ammonia-coal co-firing in a pilot-scale fluidized bed reactor: Influence of ammonia addition for emissions control. Energy Convers Manag. 2022; https://doi.org/10.1016/j.enconman.2022.115226
[18] Stocks M, Fazeli R, Hughes L, Beck FJ. Global emissions implications from co-combusting ammonia in coal fired power stations: An analysis of the Japan-Australia supply chain. J Clean Prod. 2022; https://doi.org/10.1016/j.jclepro.2021.130092
[19] Valera-Medina A, Xiao H, Owen-Jones M, David WIF, Bowen PJ. Ammonia for power. Prog Energy Combust Sci. 2018; https://doi.org/10.1016/j.pecs.2018.07.001
[20] Tamura M, Gotou T, Ishii H, Riechelmann D. Experimental investigation of ammonia combustion in a bench scale 1.2 MW-thermal pulverised coal firing furnace. Appl Energy. 2020; https://doi.org/10.1016/j.apenergy.2020.115580
[21] Ouyang Z, Liu W, Man C, Zhu J, Liu J. Experimental study on combustion, flame and NOX emission of pulverized coal preheated by a preheating burner. Fuel Process Technol. 2018; https://doi.org/10.1016/j.fuproc.2018.07.008
[22] Kim W, Lee D, Park S. Experimental study on optimization of over-fire air in modified combustion condition with selective catalytic reduction. J Mech Sci Technol. 2011; https://doi.org/10.1007/s12206-011-0208-3
[23] Lee H, Lee M. Recent Advances in Ammonia Combustion Technology in Thermal Power Generation System for Carbon Emission Reduction. Energies. 2021; https://doi.org/10.3390/en14185604
[24] Pestheruwe N, Huangwei Z, Lin M, Ruoyang Y. Numerical simulations on the combustion and emission characteristics of a non-premixed NH3/CH4 swirling flame using LES-FGM method. AIAA SCITECH Forum. 2023. https://doi.org/10.2514/6.2023-1722
[25] Dounia O, Vermorel O, Misdariis A, Poinsot T. Influence of kinetics on DDT simulations. Combustion and Flame. 2019. https://doi.org/10.1016/j.combustflame.2018.11.009
[26] Taamallah S, Vogiatzaki K, Alzahrani FM, Mokheimer EM, Habib MA, Ghoniem AF. Fuel flexibility, stability and emissions in premixed hydrogen-rich gas turbine combustion: Technology, fundamentals, and numerical simulations. Applied energy. 2015. https://doi.org/10.1016/j.apenergy.2015.04.044
[27] Meloni R, Nassini PC, Andreini A. Model development for the simulation of the hydrogen addition effect onto the NOx emission of an industrial combustor. Fuel. 2022. https://doi.org/10.1016/j.fuel.2022.125278
[28] Zheng K, Yu M, Liang Y, Zheng L, Wen X. Large eddy simulation of premixed hydrogen/methane/air flame propagation in a closed duct. International Journal of

Hydrogen Energy. 2018. https://doi.org/10.1016/j.ijhydene.2018.01.045
[29] Rahman MN, Othman NF. A Numerical Model for Ash Deposition Based on Actual Operating Conditions of a 700 MW Coal-Fired Power Plant: Validation Feedback Loop via Structural Similarity Indexes (SSIMs). CFD Lett. 2022; https://doi.org/10.37934/cfdl.14.1.99111
[30] Rahman MN. Optimisation of Solid Fuel In-furnace Blending for an Opposed-firing Utility Boiler: A Numerical Analysis. CFD Lett. 2022; https://doi.org/10.37934/cfdl.14.9.89107
[31] Sun W, Zhong W, Echekki T. Large eddy simulation of non-premixed pulverized coal combustion in corner-fired furnace for various excess air ratios. Appl Math Model. 2019; https://doi.org/10.1016/j.apm.2019.05.017
[32] Wan K, Xia J, Wang Z, Pourkashanian M, Cen K. Large-eddy Simulation of Pilot-assisted Pulverized-coal Combustion in a Weakly Turbulent Jet. Flow Turbulence Combust. 2017; https://doi.org/10.1007/s10494-017-9817-y
[33] Sun W, Zhong W, Zhang J, Echekki T. Large Eddy Simulation on the Effects of Coal Particles Size on Turbulent Combustion Characteristics and NOx Formation Inside a Corner-Fired Furnace. J Energy Resour Technol. 2021; https://doi.org/10.1115/1.4048864
[34] Silva VB, João C. Computational fluid dynamics applied to waste to energy processes: a hands-on approach. Butterworth-Heinemann; 2020.
[35] Hu Y, Naito S, Kobayashi N, Hasatani M. CO2, NOx and SO2 emissions from the combustion of coal with high oxygen concentration gases. Fuel. 2000; https://doi.org/10.1016/S0016-2361(00)00047-8
[36] Askarova AS, Messerle VE, Ustimenko AB, Bolegenova SA, Maximov VY, Yergalieva AB. Reduction of noxious substance emissions at the pulverized fuel combustion in the combustor of the BKZ-160 boiler of the Almaty heat electropower station using the "Overfire Air" technology*. Thermophys Aeromechanics. 2016; https://doi.org/10.1134/S0869864316010133
[37] Speight JG. Coal-fired power generation handbook. John Wiley & Sons; 2021. ISBN: 978-1-119-51013-0
[38] Nagatani G, Ishii H, Ito K, Ohno E, Okuma Y. Development of Co-Firing Method of Pulverized Coal and Ammonia to Reduce Greenhouse Gas Emissions. IHI Engineering Review. 2020. https://www.ihi.co.jp/en/technology/sdgs/topic01/pdf/Vol53No1_F.pdf

Abbreviations

CFD	Computational Fluid Dynamics
COP26	UN's Climate Change Conference
IGCC	Integrated Gasification Combined Cycle
CCS	Carbon Capture and Storage
UC	Unburned carbon
ASR	Air Staging Ratio
TM	Total moisture
FC	Fixed carbon
GCV	Gross Calorific Value
H	Hydrogen element
O	Oxygen element
OFA	Over-fire Air
PA	Primary Air
DO	Discrete Ordinate
HCN	Hydrogen Cyanide
CO	Carbon Monoxide
H_2S	Hydrogen Sulphide
CS_2	Carbon Disulphide
NO_x	Nitrogen Oxides
NH_3	Ammonia
SO_2	Sulphur Dioxide
CO_2	Carbon Dioxide
SA	Secondary Air
LPG	Liquefied Petroleum Gas
VM	Volatile matter
AC	Ash content
C	Carbon element
N	Nitrogen element
S	Sulphur element
NS	Navier–Stokes
LES	Large Eddy Simulation
WSGGM	Weighted-sum-of-gray-gases Model
OH	Hydroxide
ad	Air-dried basis
COS	Carbonyl Sulphide